PHYSICAL REVIEW D **84,** 056004 (2011)

QCD phase diagram from finite energy sum rules

Alejandro Ayala,[1] Adnan Bashir,[2] C. A. Dominguez,[3] Enif Gutiérrez,[2] M. Loewe,[4] and Alfredo Raya[2]

[1]*Instituto de Ciencias Nucleares, Universidad Nacional Autónoma de México, Apartado Postal 70-543, México Distrito Federal 04510, Mexico*

[2]*Instituto de Física y Matemáticas, Universidad Michoacana de San Nicolás de Hidalgo, Edificio C-3, Ciudad Universitaria, Morelia, Michoacán 58040, Mexico*

[3]*Centre for Theoretical Physics and Astrophysics, University of Cape Town, Rondebosch 7700, South Africa and Department of Physics, Stellenbosch University, Stellenbosch 7600, South Africa*

[4]*Pontificia Universidad Católica de Chile, Facultad de Física, Casilla 306, Santiago 22, Chile*

(Received 25 June 2011; published 6 September 2011)

We study the QCD phase diagram at finite temperature and baryon chemical potential by relating the behavior of the light-quark condensate to the threshold energy for the onset of perturbative QCD. These parameters are connected to the chiral symmetry restoration and the deconfinement phase transition, respectively. This relation is obtained in the framework of finite energy QCD sum rules at finite temperature and density, with input from Schwinger-Dyson methods to determine the light-quark condensate. Results indicate that both critical temperatures are basically the same within some 3% accuracy. We also obtain bounds for the position of the critical end point, $\mu_{Bc} \gtrsim 300$ MeV and $T_c \lesssim 185$ MeV.

DOI: 10.1103/PhysRevD.84.056004 PACS numbers: 25.75.Nq, 11.15.Tk, 11.30.Rd, 11.55.Hx

I. INTRODUCTION

In quantum chromodynamics (QCD), the strong interaction among quarks depends on their color charge. When quarks are placed in a medium, this color charge is screened with increasing density. The density can increase either by raising the temperature, so that collisions between quarks produce more quarks and gluons, or by compressing the system, thereby increasing the baryon density. If the density increases beyond a certain critical value, one expects that the interactions between quarks no longer confine them inside a hadron, so that they are free to travel longer distances and deconfine. This transition from a confined to a deconfined phase is usually referred to as the *deconfinement phase transition*.

A separate phase transition takes place when the realization of chiral symmetry shifts from a Nambu-Goldstone phase to a Wigner-Weyl phase. In the massless quark limit, this is achieved by the vanishing of the quark condensate, or alternatively the pion decay constant. Qualitatively, one expects these two phase transitions to take place at approximately the same temperature. An outstanding issue is whether this conclusion also holds quantitatively. To address this, it has been customary to study the behavior of the order parameters of these transitions as functions of the temperature T and the baryon chemical potential μ_B, namely, the Polyakov loop L [1] and quark antiquark condensate $\langle \bar{\psi}\psi \rangle$ in the chiral limit, respectively. In the confined phase, the former parameter either vanishes in the limit of massless quarks, or else it is exponentially suppressed for finite quark masses, while it is finite in the deconfined phase. The quark condensate is finite in the broken chiral-symmetry phase, while it vanishes in the chirally symmetric phase at high enough temperature, and in the limit of massless quarks. For finite quark masses chiral symmetry is explicitly broken at the Lagrangian level and therefore the phase transition is suppressed. This is similar to what happens to a ferromagnet in the presence of an external magnetic field. In this situation one might need to specify to what extent one is still dealing with a phase transition.

At finite T, and $\mu_B = 0$, lattice QCD calculations provide a consistent quantitative picture of the above behavior, resulting in similar critical temperatures T_c for both transitions in the range 170 MeV $\lesssim T_c \lesssim$ 200 MeV, for finite quark masses [2–4]. The situation is much less clear cut when both T and μ_B are simultaneously nonzero. Lattice QCD simulations cannot be used for $\mu_B \neq 0$ because the fermion determinant becomes complex and thus standard Monte Carlo methods fail, as the integrand is no longer real and positive definite. However, these techniques can still be adapted to extract some, though not exact, information on the QCD phase diagram for $\mu_B \neq 0$ [5]. Therefore, one needs to resort either to mathematical constructions to overcome the above limitation [6], or to model calculations [7]. Of particular recent interest is the search for a possible critical end point [8] that signals the strengthening of the order of the transition with increasing μ_B, indicating the beginning of a true chiral symmetry restoring/deconfining phase transition. The results from Monte Carlo simulations and model calculations, with and without Polyakov loop, or its variants, seem to be in conflict. In fact, the former give smaller (larger) values for the end point baryon chemical potential (temperature) than the latter. Things become worse if one uses the imaginary chemical potential method, a well established technique for not too large values of μ_B. Indeed, this leads to a shrinking and

weakening region of chiral phase transitions with increasing μ_B, thus suggesting that there is no critical end point for $\mu_B \lesssim 500$ MeV [9]. It has also been pointed out that even if the transition weakens with increasing μ_B, the existence of the critical end point would not be ruled out, although it would require a nonmonotonic behavior [10]. In view of this situation, alternative ways of examining the QCD phase diagram are required.

One possibility is to look at variables that describe deconfinement other than the Polyakov loop. A phenomenological QCD parameter associated with deconfinement was first proposed long ago in [11], and it is the square energy (s_0) beyond which the hadronic resonance spectral function becomes smooth and well described by perturbative QCD (PQCD). At $T = 0$ this continuum threshold lies in the range $s_0 \simeq 1$–3 GeV^2, depending on the channel. At finite temperature one expects s_0 to decrease with increasing T and approach the kinematical threshold at some critical value $T = T_c$, to be identified with the deconfinement temperature. In this scenario one expects stable particles (poles on the real axis in the complex squared energy s-plane) to develop a width as a result of absorption in the thermal bath. At the same time, resonances (poles in the second Riemann sheet in the complex s-plane) should develop T-dependent widths, increasing with increasing temperature. Such a *resonance broadening* mechanism was first proposed in detail in connection with dimuon production in heavy ion collisions [12].

The natural framework to determine s_0 has been that of QCD sum rules [13]. This quantum field theory framework is based on the operator product expansion (OPE) of current correlators at short distances, extended beyond perturbation theory, and on Cauchy's theorem in the complex s-plane. The latter is usually referred to as quark-hadron duality. Vacuum expectation values of quark and gluon field operators effectively parametrize the effects of confinement. An extension of this method to finite temperature was first outlined in [11]. Further evidence supporting the validity of this program was provided in [14], followed by a large number of applications [15,16]. Of particular interest to the present work are the results obtained for $s_0(T)$ in [15] using QCD finite energy sum rules (FESR) for the (light-quark) axial-vector current correlator. The leading dimension FESR relates $s_0(T)$ to the pion decay constant $f_\pi(T)$, and this in turn to the light-quark condensate (using the Gell-Mann-Oakes-Renner relation [17]). In the chiral limit it was found that $s_0(T)/s_0(0) \simeq f_\pi(T)/f_\pi(0) \simeq \langle\bar{\psi}\psi\rangle \times (T)/\langle\bar{\psi}\psi\rangle(0)$, which holds to a very good approximation. This relation hints towards the possible coincidence of the critical temperatures for deconfinement and chiral symmetry restoration. In this paper, we extend this analysis to finite density, thus obtaining $s_0(T, \mu_B)$ from FESR using as input the light-quark condensate at finite temperature and density determined in the Schwinger-Dyson equations (SDE) framework.

The paper is organized as follows: In Sec. II, we find the relation between the quark condensate and the PQCD threshold s_0 using FESR for the axial-vector current correlator. In Sec. III, we compute the quark condensate at finite T and μ_B from a convenient parametrization of the quark propagator in the SDE framework. In Sec. IV, we present our analysis of the QCD phase diagram and show that the deconfinement and chiral symmetry restoration transitions take place at basically the same temperature to some 3% accuracy, i.e. within the numerical precision of the method. We finally summarize and discuss our results in Sec. V.

II. FINITE ENERGY QCD SUM RULES

We begin by considering the (charged) axial-vector current correlator at $T = 0$

$$\Pi_{\mu\nu}(q^2) = i\int d^4x e^{iq\cdot x}\langle 0|T(A_\mu(x)A_\nu(0))|0\rangle, \\ = -g_{\mu\nu}\Pi_1(q^2) + q_\mu q_\nu \Pi_0(q^2), \tag{1}$$

where $A_\mu(x) =: \bar{u}(x)\gamma_\mu\gamma_5 d(x)$: is the axial-vector current, $q_\mu = (\omega, \vec{q})$ is the four-momentum transfer, and the functions $\Pi_{0,1}(q^2)$ are free of kinematical singularities. Concentrating on the function $\Pi_0(q^2)$ and writing the OPE beyond perturbation theory in QCD [13], one of the two pillars of the sum rule method, one has

$$\Pi_0(q^2)|_{\rm QCD} = C_0\hat{I} + \sum_{N=1} C_{2N}(q^2, \mu^2)\langle\hat{\mathcal{O}}_{2N}(\mu^2)\rangle, \tag{2}$$

where μ^2 is a renormalization scale, the Wilson coefficients C_N depend on the Lorentz indices and quantum numbers of the currents and on the local gauge invariant operators $\hat{\mathcal{O}}_N$ built from the quark and gluon fields in the QCD Lagrangian. These operators are ordered by increasing dimensionality and the Wilson coefficients, calculable in PQCD, fall off by corresponding powers of $-q^2$. The unit operator above has dimension $d = 0$ and $C_0\hat{I}$ stands for the purely perturbative contribution. Hence, this OPE factorizes short distance physics, encapsulated in the Wilson coefficients, and long distance effects parametrized by the vacuum condensates. The second pillar of the QCD sum rule technique is Cauchy's theorem in the complex squared energy s-plane

$$\frac{1}{\pi}\int_0^{s_0} ds f(s)\mathrm{Im}\Pi_0(s) = -\frac{1}{2\pi i}\oint_{C(|s_0|)} ds f(s)\Pi_0(s), \tag{3}$$

where $f(s)$ is an arbitrary analytic function, and the radius of the circle s_0 is large enough for QCD and the OPE to be used on the circle (see Fig. 1). The integral along the real s-axis involves the hadronic spectral function. This equation is the mathematical statement of what is usually referred to as *quark-hadron duality*. Using the OPE,

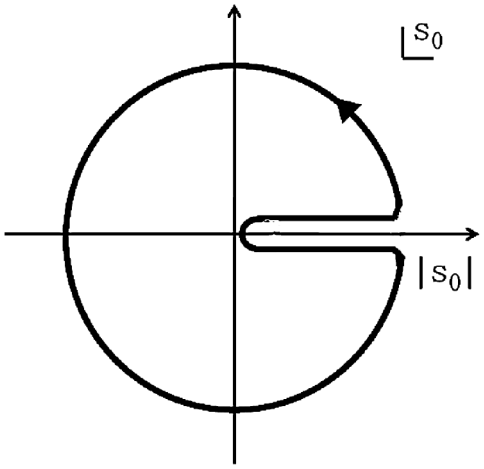

FIG. 1. FESR integration contour $C(|s_0|)$ in the complex square energy s-plane. The QCD threshold s_0 in the FESR is the radius of the circle.

Eq. (2), and an integration kernel $f(s) = s^N (N = 1, 2, \cdots)$ one obtains the FESR

$$(-)^{N-1} C_{2N} \langle \hat{\mathcal{O}}_{2N} \rangle = 4\pi^2 \int_0^{s_0} ds s^{N-1} \frac{1}{\pi} \mathrm{Im}\Pi_0(s) - \frac{s_0^N}{N}[1 + \mathcal{O}(\alpha_s)] (N = 1, 2, \cdots). \quad (4)$$

For $N = 1$ the dimension $d = 2$ term in the OPE does not involve any condensate, as it is not possible to construct a gauge invariant operator of such a dimension from the quark and gluon fields. Nevertheless, it is a priori conceivable to generate a $d = 2$ term in some dynamical fashion, e.g. in PQCD at very high order (renormalons). However, there is no evidence for such a term (at $T = 0$) from FESR analyses of experimental data on e^+e^- annihilation and τ decays into hadrons [18]. At very high temperatures, though, there seems to be evidence for some $d = 2$ term [19]. However, the analysis to be reported here is performed at much lower values of T, so that we can safely ignore this contribution in the sequel.

The extension of this program to finite temperature is fairly straightforward [11,14], with the Wilson coefficients in the OPE, Eq. (2), remaining independent of T at leading order in α_s, and the condensates developing a temperature dependence. Radiative corrections in QCD involve now an additional scale, i.e. the temperature, so that $\alpha_s \equiv \alpha_s(\mu^2, T)$. This problem has not yet been solved successfully. Nevertheless, from the size of radiative corrections at $T = 0$ one does not expect any major loss of accuracy in results from thermal FESR to leading order in PQCD, as long as the temperature is not too high, say $T \lesssim 200$ MeV. Essentially, all applications of FESR at $T \neq 0$ have been done at leading order in PQCD, thus implying a systematic uncertainty at the level of 10%. One new feature at $T \neq 0$ is the appearance of a new cut in the complex energy ω-plane [11], and centered at the origin with extension $-|\vec{q}| \leq \omega \leq |\vec{q}|$. This is due to a contribution to the current correlator in the spacelike region ($q^2 < 0$) which vanishes at $T = 0$. Conceptually, this originates in the scattering of the current by either quarks (antiquarks) or by hadrons in the medium, in the case of QCD or the hadronic representation, respectively. When considering the rest-frame ($\vec{q} \to 0$), this scattering term either becomes a delta function of the energy or it vanishes identically, depending on the channel. For instance, in the case of the axial-vector current correlator, Eq. (1), the QCD scattering term is proportional to $\delta(\omega^2)$. The corresponding term in the hadronic representation is nonzero, but it is suppressed relative to the tree-level pion contribution, as the axial-vector current can only couple to an odd number of pions. Another new feature at finite temperature is the possible existence of nonscalar (Lorentz noninvariant) vacuum condensates. This does not affect the present analysis, as we shall only consider dimension $d = 2$ FESR.

In the static limit ($\vec{q} \to 0$), to leading order in PQCD, and for $T \neq 0$ and $\mu_q \neq 0$, where $\mu_q = \mu_B/3$ is the quark chemical potential, the function $\Pi_0(q^2)$ in Eq. (1) becomes $\Pi_0(\omega^2, T, \mu_q)$; to simplify the notation we shall omit the T and μ_q dependence in the sequel. A straightforward calculation of the spectral function in perturbative QCD gives

$$\frac{1}{\pi} \mathrm{Im}\Pi_0(s)|_{\mathrm{PQCD}} = \frac{1}{4\pi^2}\left[1 - \tilde{n}_+\left(\frac{\sqrt{s}}{2}\right) - \tilde{n}_-\left(\frac{\sqrt{s}}{2}\right)\right] - \frac{2}{\pi^2} T^2 \delta(s)[\mathrm{Li}_2(-e^{\mu_q/T}) + \mathrm{Li}_2(-e^{-\mu_q/T})], \quad (5)$$

where $\mathrm{Li}_2(x)$ is the dilogarithm function, $s = \omega^2$, and

$$\tilde{n}_{\pm}(x) = \frac{1}{e^{(x \mp \mu_q)/T} + 1} \quad (6)$$

are the Fermi-Dirac thermal distributions for particles and antiparticles, respectively. We have assumed massless quarks, as quark mass corrections are negligible.

In the limit where T and/or μ_q are large with respect to a given mass scale such as the quark mass, Eq. (5) becomes

$$\frac{1}{\pi} \mathrm{Im}\Pi_0(s)|_{\mathrm{PQCD}} = \frac{1}{4\pi^2}\left[1 - \tilde{n}_+\left(\frac{\sqrt{s}}{2}\right) - \tilde{n}_-\left(\frac{\sqrt{s}}{2}\right)\right] + \frac{1}{\pi^2}\delta(s)\left(\mu_q^2 + \frac{\pi^2 T^2}{3}\right). \quad (7)$$

In the hadronic sector, we assume pion-pole dominance of the hadronic spectral function, i.e. the continuum threshold s_0 to lie below the first radial excitation with mass $M_{\pi_1} \simeq 1300$ MeV. This is a very good approximation at finite T, as we expect s_0 to be monotonically decreasing with increasing temperature. In this case,

$$\frac{1}{\pi}\,\mathrm{Im}\Pi(s)|_{\mathrm{HAD}} = 2f_\pi^2(T,\mu_q)\delta(s), \tag{8}$$

where $f_\pi(T,\mu_q)$ is the pion decay constant at finite T and μ_q, with $f_\pi(0,0) = 92.21 \pm 0.14$ MeV [20].

Turning to the FESR, Eq. (4), with $N = 1$ and no dimension $d = 2$ condensate, and using Eqs. (5) and (8), one finds

$$\int_0^{s_0(T,\mu_q)} ds\left[1 - \tilde{n}_+\left(\frac{\sqrt{s}}{2}\right) - \tilde{n}_-\left(\frac{\sqrt{s}}{2}\right)\right] = 8\pi^2 f_\pi^2(T,\mu_q) + 8T^2[\mathrm{Li}_2(-e^{\mu_q/T}) + \mathrm{Li}_2(-e^{-\mu_q/T})] \tag{9}$$

This is a transcendental equation determining $s_0(T,\mu_q)$ in terms of $f_\pi(T,\mu_q)$. The latter is related to the light-quark condensate through the Gell-Mann-Oakes-Renner relation [17]

$$\frac{f_\pi^2(T,\mu_q)}{f_\pi^2(0,0)} = \frac{\langle\bar{\psi}\psi\rangle(T,\mu_q)}{\langle\bar{\psi}\psi\rangle(0,0)}, \tag{10}$$

where the quark and pion masses have been assumed independent of T and μ_q [21]. A good closed form approximation to the FESR, Eq. (9), for large T and/or μ_q is obtained using Eq. (7) with $\tilde{n}_+(\frac{\sqrt{s}}{2}) \simeq \tilde{n}_-(\frac{\sqrt{s}}{2}) \simeq 0$, in which case

$$s_0(T,\mu_q) \simeq 8\pi^2 f_\pi^2(T,\mu_q) - \frac{4}{3}\pi^2 T^2 - 4\mu_q^2. \tag{11}$$

Using Eq. (10), this can be rewritten as

$$\frac{s_0(T,\mu_q)}{s_0(0,0)} \simeq \frac{\langle\bar{\psi}\psi\rangle(T,\mu_q)}{\langle\bar{\psi}\psi\rangle(0,0)} - \frac{(T^2/3 - \mu_q^2/\pi^2)}{2f_\pi^2(0,0)}. \tag{12}$$

The quark condensate can be computed from the in-medium quark propagator, whose nonperturbative properties can be obtained e.g. from known solutions to the Schwinger-Dyson equations (SDE) as discussed in the next section.

III. QUARK PROPAGATOR AND CONDENSATE

The quark condensate can be computed from the quark propagator $S(k_0,\vec{k})$ in Euclidean space. At finite T and μ_q the condensate is given by

$$\begin{aligned}\langle\bar{\psi}\psi\rangle(T,\mu_q) &= -N_c T\sum_n\int\frac{d^3k}{(2\pi)^3}\,\mathrm{Tr}S[(2n+1)\pi T + i\mu_q,\vec{k}] \\ &= -N_c T\sum_n\int\frac{d^4k}{(2\pi)^3}\,\mathrm{Tr}[S(k_0,\vec{k})] \\ &\quad\times\delta[k_0 - (2n+1)\pi T - i\mu_q].\end{aligned} \tag{13}$$

Introducing the Poisson summation formula

$$\sum_l(-1)^l\exp\{(ik_0+\mu_q)l/T\} = (2\pi)T\sum_n\delta[k_0 - (2n+1)\pi T - i\mu_q], \tag{14}$$

leads to

$$T\sum_n\int\frac{d^3k}{(2\pi)^3}\,\mathrm{Tr}S[(2n+1)\pi T + i\mu_q,\vec{k}] = \sum_l(-1)^l\int\frac{d^4k}{(2\pi)^4}\,\mathrm{Tr}[S(k_0,\vec{k})]\exp\{(ik_0+\mu_q)l/T\}. \tag{15}$$

Using this result in Eq. (13) gives

$$\langle\bar{\psi}\psi\rangle(T,\mu_q) = -N_c\sum_l(-1)^l\int\frac{d^4k}{(2\pi)^4}\,\mathrm{Tr}[S(k_0,\vec{k})] \times\exp\{(iq_0+\mu_q)l/T\}. \tag{16}$$

Notice that from Eq. (16), the vacuum contribution to the condensate comes from the term with $l = 0$. For this, we use the value

$$\langle\bar{\psi}\psi\rangle|_0 = -(0.241\ \mathrm{GeV})^3. \tag{17}$$

The true matter contribution to the condensate is thus

$$\langle\bar{\psi}\psi\rangle(T,\mu_q) = -N_c\sum_{l\neq0}(-1)^l\int\frac{d^4k}{(2\pi)^4}\,\mathrm{Tr}[S(k_0,\vec{k})] \times\exp\{(iq_0+\mu_q)l/T\}. \tag{18}$$

Because of the loss of Lorentz covariance at finite T and/or μ_q, the general structure of the propagator is given by

$$S^{-1}(k_0,\vec{k}) = A\gamma_0 k_0 + B\vec{\gamma}\cdot\vec{k} + C, \tag{19}$$

where A, B and C are scalar functions of k_0 and $\vec{k}$. They can be obtained from nonperturbative methods such as solutions to SDE. We adopt this procedure here. Motivated by the success of the rainbow-ladder truncation of the SDE and the effective interaction of Ref. [22] in the description of light pseudoscalar and vector mesons, and the meromorphic representation of the quark propagator [23], we consider the parametrization

$$S(k_0,\vec{k}) = \sum_{i=1}^{3}\left(\frac{r_i}{ik + m_i}\right) + \frac{r_4}{i\gamma_0 k_0 + ib\vec{\gamma}\cdot\vec{k} + m_4}, \tag{20}$$

and choose b, the masses m_i, and the residues r_i, $i = 1\ldots4$, to be real numbers. In addition we seek T-dependent values of b, m_4 and r_4. The Lorentz covariant part of this parametrization is fitted by requiring the propagator to reproduce key features of the rainbow-ladder model [22] at $T = 0$. In particular, to match the ultraviolet behavior of the gap equation for massive u/d quarks, the value of the condensate in vacuum, and the constituent

quark masses, as dictated by the solutions to SDE. Table I shows the values thus obtained for the parameters m_i and r_i, $i = 1 \ldots 3$. The last term in Eq. (20) is added to reproduce the Lorentz covariance breaking effects of the heat bath at $T \neq 0$ and/or $\mu_q \neq 0$. The values of b, m_4 and r_4 are adjusted to reproduce the light-quark condensate as a function of T for $\mu_B = 0$ [see Eq. (21) below] extracted from lattice QCD [3] by means of a point-distance minimization procedure over a grid of 1500 points along the T interval. Thus, these parameters are in fact nonanalytic functions of T which, in practice, are numerically interpolated to obtain the propagator. Table II shows the values of these parameters calculated at the temperatures where the lattice points are given. Carrying out the integrations in Eq. (18), and in terms of the parametrization of the quark propagator in Eq. (20), we obtain

$$\langle \bar{\psi}\psi \rangle(T, \mu_q)|_{\text{matt}} = -\frac{8TN_c}{\pi^2} \sum_{l=1}^{\infty} \frac{(-1)^l}{l} \cosh\left(\frac{\mu_q l}{T}\right) \times \sum_{i=1}^{4} \frac{r_i m_i^2}{|b_i|^3} K_1\left(\frac{l|m_i|}{T}\right), \quad (21)$$

where $K_1(x)$ is a Bessel function, and for convenience we have defined $b_i = 1$ for $i = 1, 2, 3$, and $b_4 = b$. Fig. 2 shows the lattice QCD data for the light-quark condensate as a function of T [3] together with the curve obtained from the absolute value of the sum of Eqs. (17) and (21) for $\mu_B = 0$. This parametrization gives a good description of the condensate for the range of temperatures where the phase transition occurs.

TABLE I. Parameters m_i and r_i, $i = 1, 2, 3$ to describe the Lorentz covariant part of the quark propagator.

i	m_i (GeV)	r_i
1	−0.490	−0.112
2	0.495	0.352
3	−0.879	0.259

TABLE II. Parameters b, m_4 and r_4, which describe the Lorentz breaking part of the propagators at the lattice T points.

T (GeV)	$r_4 m_4^2/b_4^3$ (GeV^2)	m_4 (GeV)
0.139	−0.0 651 954	0.366 218
0.154	−0.0 494 999	0.305 228
0.170	−0.0 377 697	0.220 547
0.175	−0.10 482	0.321 765
0.180	−0.0952 544	0.279 434
0.185	−0.352 287	0.437 673
0.191	−0.344 934	0.19 104
0.196	−0.123 177	0.250 567
0.198	−0.342 024	0.397 248
0.206	−1.39 944	0.377 043
0.219	−0.975 465	0.387 967
0.227	−0.460 765	0.489 013
0.243	−1.30 498	0.802 619
0.259	−0.851 509	0.693 332

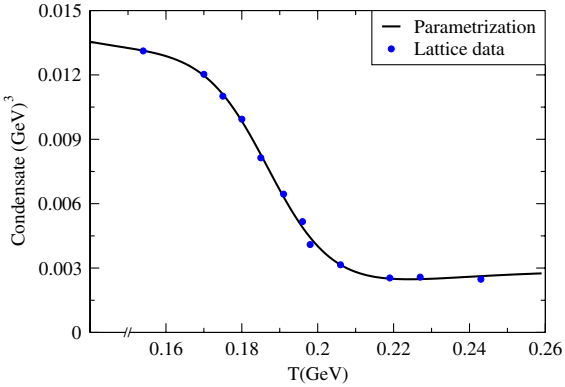

FIG. 2 (color online). (Color online) Lattice data and parametrization of the absolute value of the quark condensate as a function of T in the phase transition region.

IV. QCD PHASE DIAGRAM

With the parametrization of lattice data at finite T and $\mu_B = 0$, we proceed to extend the analysis to finite $\mu_B = 3\mu_q$. To explore the QCD phase diagram we make use of the expressions for the light-quark condensate and the PQCD threshold s_0 that describe the chiral and deconfinement phase transitions, respectively. Next, we compute the corresponding susceptibilities which are proportional to the heat capacities, $-\partial\langle\bar{\psi}\psi\rangle/\partial T$ and $-\partial s_0/\partial T$. Figs. 3 and 4 show examples of these heat capacities (normalized to their vacuum values) for two

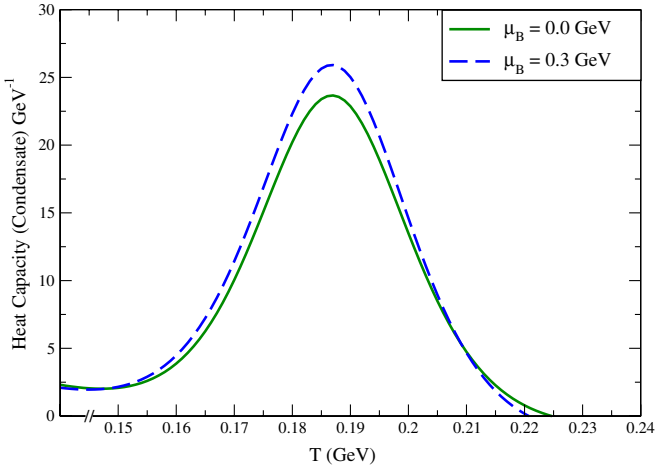

FIG. 3 (color online). (Color online) Heat capacity for the normalized (to its vacuum value) quark condensate as a function of T for $\mu_q = 0$ (solid line) and $\mu_B = 300$ MeV (dash line). The critical temperature T_c corresponds to the maximum of the heat capacity for a given value of μ_B.

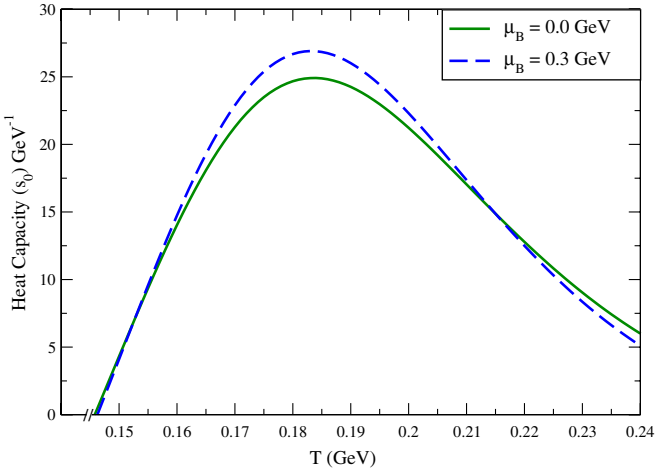

FIG. 4 (color online). (Color online) Heat capacity for the PQCD normalized (to its vacuum value) threshold energy squared s_0 as a function of T for $\mu_B = 0$ (solid line) and $\mu_B = 300$ MeV (dash line). The critical temperature T_c corresponds to the maximum of the heat capacity for a given value of μ_B.

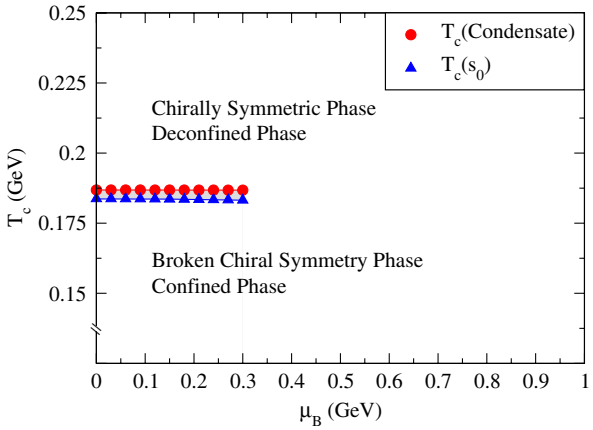

FIG. 5 (color online). (Color online) Transition temperatures for the quark condensate and the PQCD threshold energy squared s_0 as functions of the baryon chemical potential.

values of $\mu_B = 0$, 0.3 GeV. For a given μ_B, the transition temperature is identified as the value T_c where the heat capacity reaches a maximum. Fig.5 shows the transition temperatures for the condensate and for s_0. These temperatures are basically identical within a small window of roughly 3 MeV around $T = 185$ MeV, for all values of μ_B up to the maximum value of $\mu_B = 300$ MeV.

V. DISCUSSION AND CONCLUSIONS

In this paper, we have studied the QCD phase diagram at $T \neq 0$ and $\mu_B \neq 0$ based on the behavior of the light-quark condensate and of the PQCD threshold as probes of chiral symmetry restoration and deconfinement, respectively. We have shown that these quantities are related through a QCD FESR and found that they lead to essentially equal transition temperatures.

We have worked to leading order within the FESR approach. Notice that potential corrections to the factorization of short and long distance contributions in the operator product expansion can manifest in the calculation of the Wilson coefficients. The origin of such potential corrections are the extra scales introduced by T and/or μ_q, upon which the coupling constant can depend. Given the lack of theoretical insight into this problem, in this work we rely on the fact that the size of perturbative corrections at leading order for $T = 0$ is small when the scale involved is not too high, say, of order 200 MeV. If such scale is taken as T or μ_q, this means that we expect the same degree of accuracy as for $T = 0$ calculations. This places an upper limit for the ranges of T and μ_q. Since the transition temperature is below this scale, we are in a safe regime. Furthermore, the hard thermal loop approximation relies on systematically assuming that T or μ_q are larger than any mass scale in the problem. Since the only masses that are relevant are the quark or the pion mass, which we are taking as vanishing, this places a lower limit for the ranges of T and μ_q. The upshot is that there is a window $0 \lesssim T$, $\mu_q \lesssim 200$ MeV where the approximations are valid.

The quark condensate, and thus the PQCD threshold, is computed using the quark propagator in the SDE framework. We have found it convenient to use a meromorphic parametrization of this propagator in terms of real poles and residues. These are fixed by demanding consistency with the rainbow-ladder truncation of SDE at $T = 0$, and a good description of lattice QCD data for the quark condensate at finite T. With this simple scenario we have been able to extend the analysis up to baryon chemical potential $\mu_B \simeq 300$ MeV. From our results, we can estimate the position of the critical end point to be $\mu_{Bc} \gtrsim 300$ MeV and $T_c \lesssim 185$ MeV, respectively. To parametrize the quark condensate, we have made use of the lattice data provided in Ref. [3]. There are other lattice results that give a slightly lower transition temperature for $\mu_B = 0$. Most notably, the HotQCD Collaboration has recently reported the value $T_c = 157 \pm 6$ MeV using a highly improved staggered quark (HISQ) action [24]. It is clear that we can employ our approach to adjust our results to that transition temperature since all that is involved is an adjustment of the fit. A better fit, using a better representation of the quark propagator, is in order even before. Therefore, a more precise location of the critical end point requires a more refined treatment of the parametrization of the quark propagator. This is work in progress and will be reported elsewhere.

ACKNOWLEDGMENTS

We thank E. Cuautle and J. C. Arteaga for useful hints to carry out the parametrization procedure, W. Bietenholz for pointing out useful lattice results, P. C. Tandy for his

guidance on how to parametrize the quark propagator and extract quantities such as the condensate from this parametrization, and E. Swanson for useful suggestions. Support for this work has been received in part by CONACyT (Mexico) under Grants No. 82230, 128534, CIC-UMSNH 4.10, 4.22, PAPIIT-UNAM IN103811-3, and FONDECYT 1095217 (Chile), Proyecto Anillos Grant No. ACT119 (Chile), and NRF (South Africa).

[1] L. D. McLerran and B. Svetitsky, Phys. Lett. B **98**, 195 (1981).

[2] J. B. Kogut and D. K. Sinclair, Phys. Rev. D **73**, 074512 (2006); M. Cheng *et al.*, Phys. Rev. D **74**, 054507 (2006); Y. Aoki, Z. Fodor, S. D. Katz, and K. K. Szabó, Phys. Lett. B **643**, 46 (2006); Y. Aoki, S. Borsányi, S. Durr, Z. Fodor, S. D. Katz, S. Krieg, and K. K. Szabó, J. High Energy Phys. 06 (2009) 088; S. Borsányi, Z. Fodor, C. Hoelbling, S. D. Katz, S. Krieg, C. Ratti, and K. K. Szabó, J. High Energy Phys. 09 (2010) 073; S. Borsanyi *et al.*, J. High Energy Phys. 11 (2010) 077.

[3] A. Bazavov *et al.*, Phys. Rev. D **80**, 014504 (2009); M. Cheng *et al.*, Phys. Rev. D **81**, 054504 (2010).

[4] K. Kanaya, in Proc. Sci., Lattice 2010 (2010) 012.

[5] F. Karsch *et al.*, Nucl. Phys. B, Proc. Suppl. **129-130**, 614 (2004).

[6] See for example: A. Alexandru, M. Faber, I. Horváth, and K.-F. Liu, Phys. Rev. D **72**, 114513 (2005); G. Endrődi, Z. Fodor, S. D. Katz, and K. K. Szabó, J. High Energy Phys. 04 (2011) 001.

[7] See for example G. A. Contrera, M. Orsaria, and N. N. Scoccola, Phys. Rev. D **82**, 054026 (2010); See for example: C. A. de Sousa, P. Costa, M. C. Ruivo, and H. Hansen, AIP Conf. Proc. **1343**, 592 (2011).

[8] See for example: S.-x. Qin, L. Chang, H. Chen, Y.-x. Liu, and C. D. Roberts, Phys. Rev. Lett. **106**, 172301 (2011); P. K. Srivastava, S. K. Tiwari, and C. P. Singh, arXiv:1101.1151; F. Xu, T. K. Mukherjee, H. Chen, and M. Huang, Eur. Phys. J. Web Conf. **13**, 02004 (2011).

[9] O. Philipsen and Ph. de Forcrand, Nucl. Phys. **A830**, 713c (2009).

[10] J. I. Kapusta and E. S. Bowman, Proc. Sci., CPOD2009 (2009) 018.

[11] A. I. Bochkarev and M. E. Shaposnikov, Nucl. Phys. **B268**, 220 (1986).

[12] C. A. Dominguez and M. Loewe, Z. Phys. C **49**, 423 (1991).

[13] For a review see e.g. P. Colangelo and A. Khodjamirian, in *At the Frontier of Particle Physics/Handbook of QCD*, edited by M. Shifman (World Scientific, Singapore, 2001), Vol. 3, p. 1495.

[14] C. A. Dominguez and M. Loewe, Phys. Rev. D **52**, 3143 (1995).

[15] C. A. Dominguez and M. Loewe, Phys. Lett. B **233**, 201 (1989); The (near) equality of the critical temperatures for chiral symmetry restoration and deconfinement was shown analytically in A. Barducci, R. Casalbuoni, S. De Curtis, R. Gatto, and G. Pettini, Phys. Lett. B **244**, 311 (1990). These authors used a result for the thermal quark condensate valid for $0 \leq T \leq T_c$, while the first reference only made use of the low-T expansion of chiral perturbation theory, obtaining somewhat different critical temperatures.

[16] For recent applications see e.g. C. A. Dominguez, M. Loewe, and J. C. Rojas, J. High Energy Phys. 08 (2007) 040; C. A. Dominguez, M. Loewe, J. C. Rojas, and Y. Zhang, Phys. Rev. D **81**, 014007 (2010); **83**, 034033 (2011), and references therein.

[17] C. A. Dominguez, M. S. Fetea, and M. Loewe, Phys. Lett. B **387**, 151 (1996).

[18] C. A. Dominguez and K. Schilcher, Phys. Rev. D **61**, 114020 (2000); J. High Energy Phys. 01 (2007) 093.

[19] E. Megias, E. R. Arriola, and L. L. Salcedo, Phys. Rev. D **81**, 096009 (2010).

[20] K. Nakamura *et al.* (Particle Data Group), J. Phys. G **37**, 075021 (2010).

[21] T. Altherr and D. Seibert, Phys. Rev. C **49**, 1684 (1994).

[22] P. Maris and C. D. Roberts, Phys. Rev. C **56**, 3369 (1997); P. Maris and P. C. Tandy, Phys. Rev. C **60**, 055214 (1999); P. Maris and C. D. Roberts, Int. J. Mod. Phys. E **12**, 297 (2003).

[23] M. S. Bhagwat, M. A. Pichowsky, and P. C. Tandy, Phys. Rev. D **67**, 054019 (2003); R. Alkofer, W. Detmold, C. S. Fischer, and P. Maris, Phys. Rev. D **70**, 014014 (2004); N. Souchlas, J. Phys. G **37**, 115001 (2010).

[24] A. Bazavov and P. Petreczky, arXiv:1107.5027.